

Microglial Calcium Release-Activated Calcium Channel Inhibition Improves Outcome from Experimental Traumatic Brain Injury and Microglia-Induced Neuronal Death

Atsushi Mizuma,^{1,2,*} Jong Youl Kim,^{1,3,*} Rachid Kacimi,¹ Ken Stauderman,⁴
Michael Dunn,⁴ Sudarshan Hebbar,⁴ and Midori A. Yenari¹

Abstract

Store-operated Ca^{2+} entry (SOCE) mediated by calcium release-activated calcium (CRAC) channels contributes to calcium signaling. The resulting intracellular calcium increases activate calcineurin, which in turn activates immune transcription factor nuclear factor of activated T cells (NFAT). Microglia contain CRAC channels, but little is known whether these channels play a role in acute brain insults. We studied a novel CRAC channel inhibitor to explore the therapeutic potential of this compound in microglia-mediated injury. Cultured microglial BV2 cells were activated by Toll-like receptor agonists or $\text{IFN}\gamma$. Some cultures were treated with a novel CRAC channel inhibitor (CM-EX-137). Western blots revealed the presence of CRAC channel proteins STIM1 and Orai1 in BV2 cells. CM-EX-137 decreased nitric oxide (NO) release and inducible nitric oxide synthase (iNOS) expression in activated microglia and reduced agonist-induced intracellular calcium accumulation in microglia, while suppressing inflammatory transcription factors nuclear factor kappa B (NF- κ B) and nuclear factor of activated T cells (NFAT). Male C57/BL6 mice exposed to experimental brain trauma and treated with CM-EX-137 had decreased lesion size, brain hemorrhage, and improved neurological deficits with decreased microglial activation, iNOS and Orai1 and STIM1 levels. We suggest a novel anti-inflammatory approach for managing acute brain injury. Our observations also shed light on new calcium signaling pathways not described previously in brain injury models.

Keywords: calcium release-activated calcium channel; microglia; store-operated calcium entry; traumatic brain injury

Introduction

ACUTE INFLAMMATORY RESPONSES are known to worsen neurological outcomes in different acute neurological injuries,¹ including traumatic brain injury (TBI).² This response is mediated acutely by microglia, the brain's resident immune cell, and circulating leukocytes that infiltrate the injured brain. This immune signaling is, in part, mediated by calcium via the calcium release-activated calcium (CRAC) channels. The CRAC channels are involved in the regulation of internal calcium stores and are activated in response to calcium depletion of the endoplasmic reticulum (ER).³ When activated, these channels replenish the calcium stores and also provide a source of calcium for other cellular activities. These channels are present on a variety of immune cells, including microglia.^{4,5}

The CRAC channel consists of the ER-resident stromal interaction molecule-1 (STIM1) and plasma membrane Orai proteins,

with Orai1 being the major isoform seen on immune cells. The STIM1 senses reductions in ER Ca^{2+} levels, which causes it to interact with and activate Orai1, a channel that allows Ca^{2+} entry.^{6,7} Calcium entry through this channel can activate calcineurin,⁸ which, among other things, leads to upregulation of proinflammatory molecules.⁹

Past work in the area of acute brain injury has shown that the immune response associated with such insults can contribute negatively to neurological outcome, and its inhibition has been shown, at least in the laboratory, to be beneficial. Inhibition of the CRAC channel pathway is possible through calcineurin inhibitors (CNIs) such as FK506 (tacrolimus) and cyclosporine A (CsA) and has been shown to improve outcomes from experimental brain trauma and related acute neurological insults.^{10–17} Clinically available CNIs, however, are not specific to this pathway and have side effects including neurotoxicity, which may limit successful translation.^{18,19}

We present results of studies of a novel small molecule inhibitor of the CRAC channel in a model of acute brain injury. This

¹Department of Neurology, University of California, San Francisco; the San Francisco VA Medical Center, San Francisco, California.

²Department of Neurology, Tokai University School of Medicine, Isehara, Japan.

³Department of Anatomy, Yonsei University College of Medicine, Seoul, South Korea.

⁴CalciMedica Inc., La Jolla, California.

*Co-first authors.

inhibitor is selective for Orai1 CRAC channels and acts upstream of calcineurin (Fig. 1, Supplementary Fig. 1 and Supplementary Tables 1 and 2; see online supplementary material at <http://www.liebertpub.com>). We report that CRAC channel inhibition using this novel small molecule inhibitor suppressed inflammatory responses in microglia and improved neurological outcomes after experimental TBI.

Methods

Materials

Reagents were purchased from Sigma (St Louis, MO). Lipopolysaccharide (LPS; *Escherichia coli*, O26:B6) was purchased from Sigma. Peroxidase-labeled *Griffonia simplicifolia* isolectin-B4 (IB4; L2140) was purchased from Sigma. Anti-CD68 antibody (ab53444) and anti-inducible nitric oxide synthase (iNOS) antibody (ab3523) were purchased from Abcam (Cambridge, MA). Alexa Fluor 488 (A-11008), Alexa Fluor 568(A-21043), and Alexa Fluor 594 (A-21213) were purchased from Life Technologies (Mulgrave, VIC, Australia). Anti NF- κ Bp65 (SC#8808), ORA1 (SC# 68895), and STIM1 (SC#66173 used only for double labeling) antibodies were purchased from Santa Cruz Biotechnologies (Santa Cruz, CA). Antibodies against nuclear factor of activated T cells (NFAT, #34389) and STIM1 (#5668S) were obtained from Cell Signaling Technologies Inc. (Danvers, MA). 4',6-diamidino-2-phenylindole (DAPI; H-1500) was purchased from Vector (Burlingame, CA). The CRAC channel inhibitor (CM-EX-137) was kindly provided by CalciMedica (La Jolla, CA).

Cell culture

BV2 cell. The immortalized mouse microglia cell line, BV2, was cultured as described previously. These cells were exhaustively shown to exhibit many phenotypical and functional properties of reactive microglia cells and are a suitable model of neuroinflammation.^{20,21} Cells were grown and maintained in Roswell Park Memorial Institute medium (RPMI) supplemented

with 10% fetal bovine serum and antibiotics (penicillin/streptomycin, 100U/mL). Under a humidified 5% CO₂/95% air atmosphere and at 37°C, cells were plated in 75 cm² cell culture flasks (Corning, Acton, MA) and were split twice a week. For the experiments, cells were plated on six-well dishes (0.5 × 10⁵ cells/well).

Cell treatment. Cells were cultured to approximately 80% confluence, and fresh serum-free medium was added for 4–24 h before administration of LPS, Poly (I:C), IFN γ , or PMA either alone or in combination with the CRAC channel inhibitor (CM-EX-137). The CM-EX-137 was dissolved in sterile dimethyl sulfoxide (DMSO) and applied to cultures 1 h before agonist application. Control cultures received DMSO only as a vehicle.

Calcium imaging studies. Changes in intracellular free Ca²⁺ concentration were monitored using the fluorescent Ca²⁺ indicator Rhod-3 (Life Technologies, Carlsbad, CA). The BV2 cells were grown on poly-d-lysine-coated dishes. Cells were either incubated for 1 h with vehicle, LPS, or LPS in combination with the CRAC channel inhibitor. Media was removed from treated cells and washed twice in phosphate buffered saline (PBS). Cells were then incubated in loading buffer containing physiological buffer, 250 mM probenecid, Power Load Component and 2.5 μ M Rhod-3-AM (Life technologies, Carlsbad, CA) for 35 min at room temperature in dark. Cells were then washed twice in physiological buffer. Live cell fluorescence microscopy of Rhod-3 (excitation/emission 560/600 nm) was performed. Images were acquired for Rhod-3-loaded cells and collected using an inverted epifluorescence microscope (Zeiss Axiovert 40 CFL; Carl Zeiss Inc). Images were captured on a cooled CCD camera. Image acquisition and analysis were performed and visualized by fluorescence, and images were obtained on a PC computer using a Zeiss Axiovert 40 CFL fluorescence microscope with Zeiss Zhen microscope software (Zeiss Inc).

Immunofluorescence microscopy. Fluorescence immunocytochemistry was performed on cells as described previously.^{20,21} After washing, cells were fixed with acetone/methanol (1:1) for

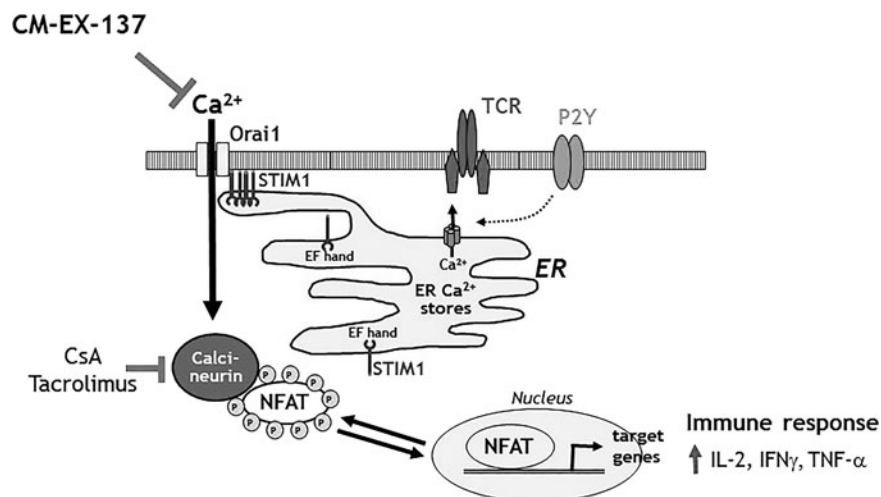


FIG. 1. Calcium release-activated calcium (CRAC) channel pathway and sites of inhibitor action. Activation of various immune receptors, including T cell receptor (TCR) and the P2Y purinergic receptors, cause release of Ca²⁺ from the endoplasmic reticulum (ER) via IP₃ receptors. The resulting decrease in ER Ca²⁺ is sensed by stromal interaction molecule-1 (STIM1), which oligomerizes and moves to positions close to the plasma membrane where it gates Orai1. Calcium entry through Orai1 then activates calcineurin, a phosphatase sensitive to cyclosporin A (CsA) and FK506 (tacrolimus). Calcineurin de-phosphorylates the transcription factor nuclear factor of activated T cells (NFAT), which then translocates to the nucleus and activates the transcription of various genes and cytokines (e.g., interleukin [IL]-2, interferon [IFN] γ , and tumor necrosis factor [TNF] α). The novel channel-selective inhibitor studied here (CM-EX-137) interacts with the CRAC channel formed by Orai1.

5 min at -20°C . Alternatively, cells were fixed in 4% paraformaldehyde (PFA) for 30 min at room temperature. After fixing, the cells were washed twice with PBS containing 0.2% Triton X-100 for 15 min. Non-specific binding sites were blocked in blocking buffer (2% bovine serum albumin [BSA] and 0.2% Triton X-100 in PBS) for 2 h. Cells were then incubated with primary antibodies selective for NF- κ B or NFAT at 1:100 dilutions in blocking buffer overnight at 4°C , followed by washing three times with blocking buffer, 10 min per wash. The cells were incubated with Alexa Fluor 488- or Alexa Fluor 594-conjugated secondary antibodies (Life Technologies), respectively, at 1:100 dilution in blocking buffer at room temperature for 1 h, then washed two times in blocking buffer and once in PBS. Fluorescence was visualized with an epifluorescence microscope (Zeiss, Carl Zeiss Inc), and images were obtained on a PC computer using Zeiss ZEN microscope software (Zeiss Inc).

Immunoblotting. At the end of the treatment period, cells were washed with cold PBS and scraped into 500 μL radio-immunoprecipitation lysis buffer with antiprotease/phosphatase and incubated for 30 min in ice with agitation as described previously.^{20,21} Lysates were sonicated and centrifuged at $10,000 \times g$ for 5 min. The supernatant was collected and either used immediately or frozen at -80°C . Protein concentration was determined using the bicinchoninic acid protein assay (Pierce, Rockford, IL), and equal amounts of protein were loaded per lane onto 10–12% sodium dodecyl sulfate-polyacrylamide gels and were electrophoresed as before. Gels were then transferred onto polyvinylidene difluoride membranes in transfer buffer containing 48 mM Tris, 150 mM glycine, and 10% methanol using a Trans-Blot apparatus (Bio-Rad, Hercules, CA) at 100 V for 1 h at 4°C . The membranes were saturated in 10 mM Tris, pH 7.4, 150 mM NaCl, 0.1% Tween-20, and 5% non-fat dry milk for 1 h at room temperature, then probed with specific antibodies for iNOS, Orai1, or STIM1 using the same buffer for 1 h at room temperature with gentle agitation.

Rabbit and mouse primary antibodies were used at working dilutions of 1:500 and 1:1000, respectively. Membranes were washed three times with 10 mM Tris, pH 7.4, 150 mM NaCl, and 0.1% Tween-20. Bound antibodies were identified after incubation with peroxidase-conjugated anti-rabbit antibodies (1:2000 dilutions in 10 mM Tris, 150 mM NaCl, 0.1% Tween buffer) for 1 h at room temperature. Membranes were then re-washed thrice, and the position of the individual proteins was detected by enhanced chemiluminescence according to the manufacturer's instructions (GE Healthcare Bioscience Corp, Piscataway, NJ).

NF- κ B and NFAT nuclear translocation. Cytoplasmic and nuclear extracts were prepared as described previously.²² NFAT and NF- κ B in nuclear extracts were evaluated by Western blot using specific antibodies for NFAT and NF- κ Bp65. We also assessed nuclear NFAT and NF- κ B translocation using immunofluorescence as described previously.²⁰

Detection of nitrite. Nitrite accumulation in media was determined as described previously.^{21,23} Briefly, BV2 cells seeded onto 6–12 well plates (2×10^5 cells/well) were cultured overnight, then switched to serum-free medium for 2–4 h, and subsequently stimulated with 1 $\mu\text{g}/\text{mL}$ LPS, Poly (I:C, 100 $\mu\text{g}/\text{mL}$), or IFN γ (100 ng/mL) with or without CM-EX-137 for 24 h. Nitric oxide (NO) was detected in the culture supernatants using the Griess assay; 50 μL of culture supernatant from each sample was transferred to a 96-well plate in triplicate, to which an equal volume of Griess reagent (Sigma-Aldrich, St. Louis, MO) was added. Absorbance was read at 540 nm on a microplate reader (Molecular Devices, Sunnyvale, CA) using Softmax Pro software analysis. After a 10 min incubation, the nitrite concentration was calculated with reference to a standard curve of freshly prepared sodium nitrite (0–100 μM).

In vivo studies

Animal protocols were approved by the institutional panel on laboratory animal care. All animal procedures were conducted in accordance with the National Institutes of Health (NIH) guidelines for the use of animals in research. Male C57/B6 mice (3–4 months of age and weighting 20–25 g, Simonsen Laboratories, Gilroy, CA) were housed and underwent a surgical procedure described in strict accordance with institutional guidelines. Forty-six mice were used in our studies as follows: sham-operated group ($n=2$), mice underwent TBI with/without CM-EX-137 treatment and survived three (22 or $n=11/\text{group}$) or 14 days (16 or $n=8/\text{group}$), and mice injected with LPS with/without CM-EX-137 (6 or $n=3/\text{group}$). Controls were treated with vehicle.

Controlled cortical impact (CCI)

The CCI to model TBI *in vivo* was performed according to a previously established protocol.²⁴ Mice were anesthetized by face mask using isoflurane (4% induction; 2% maintenance) in a mixture of $\text{O}_2:\text{N}_2\text{O}$ gases in the ratio of 2:1. The depth of anesthesia was assessed every 15 min during operation (absence of a toe pinch response, absence of any spontaneous movements, and the absence of a positive blink reflex to a puff of air directed at the eyes). Rectal temperature was maintained between $36.5\text{--}37.5^{\circ}\text{C}$ with heating pads and a lamp during operation.

Initially, anesthetized mice were fixed in a stereotaxic frame, and a midline scalp incision was made, followed by a burr hole (5 mm in diameter) in the left parietal plate immediately posterior to bregma. The dura was not disrupted. Subsequently, CCI was performed with an automated impactor (Pinpoint Precision Cortical impactor, Hatteras Instruments, Cary, NC) with a tip size of 3 mm (diameter) at 1.5 m/sec velocity to generate 2 mm penetration with a 100 msec dwell time. The excised cranial bone was replaced immediately, and the incision was then closed with suture. Mice were euthanized three days or 14 days after CCI.

Brain inflammation model

As a positive control for neuroinflammation, a separate set of mice was given LPS (5 mg/kg) by intraperitoneal (IP) injection. In this model, transient brain inflammation develops, but the animals do not have any brain cell death.²⁵ The LPS was prepared in sterile physiological saline before injection, and mice were euthanized one day after LPS injection.²⁵

CRAC channel inhibitor treatment

The same inhibitor studied in the above *in vitro* studies (CM-EX-137) was administered at a dose of 5 mg/kg/day IP starting 20 min after CCI. This treatment continued once daily for a maximum of seven days. This dosing regimen was chosen based on previous pharmacokinetic data that estimated a brain:plasma ratio of 4–5 after IP dosing and a relatively long half-life of approximately 43 h (Supplementary Fig. 2; see online supplementary material at <http://www.liebertpub.com>). Dosing continued for seven days because past work in a related model indicated that this is the period during which microglia are activated with peak numbers by 5–7 days.²⁶ The CM-EX-137 was dissolved in a sterile mixture of Carbowax 400 (NF) and pharmaceutical grade Trappsol in a 3:1 mixture. Carbowax 400/Trappsol was given as vehicle. Based on previous dose response and brain penetration studies performed by CalciMedica and pilot studies in our laboratory, the dose of 5 mg/kg CM-EX-137 was chosen to have sufficient tolerability and brain penetration after IP administration to achieve brain levels within the range that produced neuroprotection and microglial suppression in our *in vitro* studies.

Behavior studies

Neurological deficits were assessed before operation (baseline) and at one, three, seven, and 14 days after CCI, as described previously.²⁷ All tests were recorded using a video camera, and scoring was performed by two different investigators blinded to the experimental conditions.

Elevated body swing test. The elevated body swing test was performed to evaluate motor deficits. Initially, mice were suspended vertically by the tail with their heads elevated 3 inches above the test bench. A lateral swing was counted each time the animal moved its head >10 degrees away from the vertical axis. Each trial lasted 15 secs, and for each mouse, the number of right-biased swings (contralateral to the injury) was counted and compared with the total number of swings (reported as % bias). A decrease in the % bias indicated improvement.

Adhesive removal test. To estimate deficits in sensorimotor function, 50-mm² (4-mm diameter) adhesives were attached to the palm of each forepaw, and mice were observed for 2 min and scored for identifying the presence of (contact time, which estimates the ability to sense the adhesive and is thus a measure of sensory function) and removal of (removal time, which estimates motor

function) the adhesive. Shorter contact and removal times indicate improved neurological function.

Hemorrhage size. Hemorrhage size was assessed three days after CCI ($n=8$ /group). This time point was used because hemorrhage size is difficult to assess at later times because of resorption of blood. On sacrifice, mice were transcardially perfused with PBS. Brains were removed quickly, submerged in PBS, and cut into 2 mm-thick sections. Gross brain sections were scanned using a Hewlett-Packard Scanjet. Hemorrhage volumes were digitally quantified using an ImageJ (v. 1.31; publicly available through NIH), as reported previously by our group.²⁸ We estimated the total area of brain occupied by any blood multiplied by the section thickness (hemorrhage volume).

Lesion size. Lesion size was assessed 14 days after CCI from cresyl violet-stained brain sections ($n=8$ /group). On sacrifice, mice were perfused with PBS and 4% PFA. Brains were removed, fixed in PFA overnight, and subsequently cryoprotected by sinking them in increasing concentrations of sucrose (5–20%). Brains were then frozen and cut into 25 μ m thick sections on a cryostat. The six centermost sections containing the bulk of the lesion were taken for further investigation and were averaged to approximate lesion size

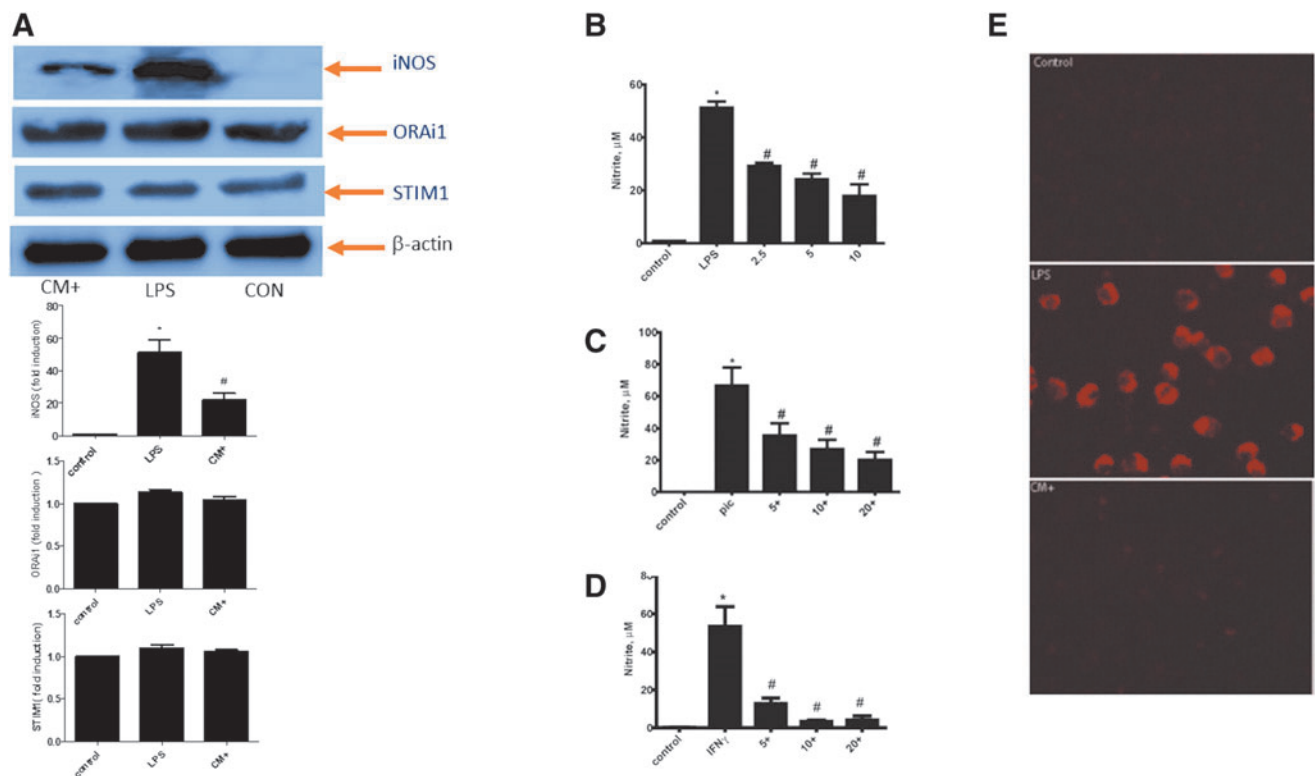


FIG. 2. Calcium release-activated calcium (CRAC) channel inhibition in cultured microglia. Microglial BV2 cells were stimulated with either lipopolysaccharide (LPS) 1 μ g/mL, Poly (I:C [PIC], 100 μ g/mL), or interferon [IFN] γ (100 ng/mL) with increasing doses of the CRAC channel inhibitor (1–20 μ M, CM-EX-137) for 24 h. (A) Western blots show constitutive expression of CRAC channel components stromal interaction molecule-1 (STIM1) and Orail. The STIM1 and Orail were not affected by LPS exposure, and these changes in protein expression were prevented by treatment with CM-EX-137 (CM+). Similar patterns of reduced protein expression were observed for proinflammatory agonists PMA, IFN γ , and PIC (not shown). Inducible nitric oxide synthase (iNOS), as a measure of microglial activation, was increased by LPS and decreased by CM-EX-137. (B) Nitric oxide accumulation is inhibited in a dose-dependent manner by CM-EX-137 after LPS exposure. (C,D) Similar dose dependency was observed when BV2 cells were stimulated by PIC (C) and by IFN γ (D). (E) CRAC channel inhibition blunts LPS-induced calcium in BV2 cells. Increased intracellular Ca²⁺ concentration was documented in cultured microglial BV2 cells after exposure to LPS. When CM-EX-137 was added to the LPS-treated microglia (CM+), the LPS-induced increase of intracellular Ca²⁺ was almost completely prevented. Unmanipulated BV2 cells are shown for comparison (Control). Data are shown as mean \pm standard error of the mean of 3–5 experiments. $p < 0.05$ * vs. control, # vs. LPS.

relative to the ipsilateral hemisphere according to a previously established protocol.^{24,27}

Histochemistry and fluorescence microscopy

For immunohistochemistry and immunofluorescence, an additional three brains/group were assessed three days post-CCI. Brains were frozen and cut into 15 μ m thick sections on a cryostat. After fixing with 4% PFA for 15 min, sections were reacted with 0.5% Triton X-100 for 10 min at room temperature, blocked with 2% normal goat serum in PBS for 1 h at room temperature, then incubated overnight at 4°C with primary antibodies in PBS or blocking solution, followed by secondary antibody. Antigen retrieval was used for STIM1 and Orai1 staining, employing 0.1% trypsin-ethylenediaminetetraacetic acid for 30 min at 37°C before incubation with the primary antibody.

Immunohistochemistry. Microglia were identified by lectin histochemistry. Sections were blocked with 2% normal goat serum in PBS, followed by incubation in 0.3% H₂O₂ for 5 min at room temperature. Sections were incubated in peroxidase-labeled IB4, then colorized with diaminobenzidine (Vector Laboratories, Burlingame, CA) and counterstained with hematoxylin. The images were captured on a PC computer using a microscopy camera (INFINITY2; Lumenera, Ottawa, Ontario, Canada).

Immunofluorescence. The following primary antibodies and concentrations were used: anti-CD11b (1:200), anti-CD68 antibody (1:50 dilution), and anti-iNOS antibody (1:200 dilution). After incubating in primary antibodies overnight, sections were incubated with secondary antibody (Alexa Fluor 594 for CD68 and Alexa Fluor 488 for iNOS) at 1:200 dilution in blocking solution for 1 h at room temperature. The STIM1 and Orai1 activation were also assessed by double staining. The following primary antibodies/concentrations—anti-STIM1 antibody at 1:50 dilution and anti-Orai1 antibody at 1:50 dilution—plus anti-CD11b antibody at 1:200 dilution were incubated with secondary antibody (Alexa Fluor 568/488 for STIM1/CD11b and Alexa Fluor 488/568 for Orai1/CD11b) at 1:200 dilution in blocking solution for 1 h at room temperature. Sections were rinsed with PBS three times, 5 min each; DAPI was used to stain cell nuclei. The images were visualized with an epifluorescence microscope (Zeiss Axiovert; Carl Zeiss) and captured on a PC computer using Axiomatic software (ZEN lite; Zeiss). Images were visualized and captured using laser confocal microscopy (LSM510, Zeiss).

Cell counting

Positive cells and DAPI-stained nuclei were counted using ImageJ software. Counts were performed using methods published previously by our group.²² Activated microglia were counted from immunopositive cells (IB4, CD68, iNOS, and CD11b), which also

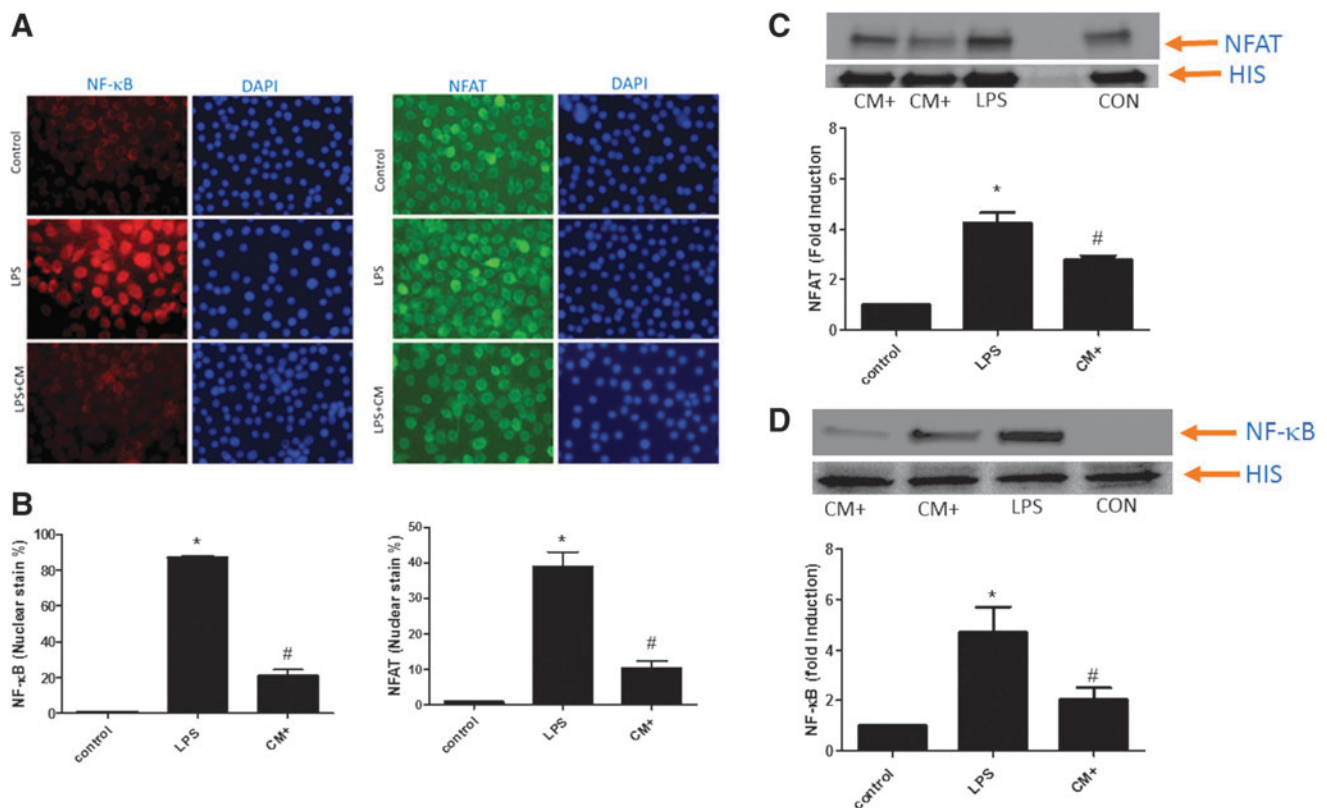


FIG. 3. Calcium release-activated calcium (CRAC) channel inhibition prevents lipopolysaccharide (LPS)-induced NF- κ B and nuclear factor of activated T cells (NFAT) nuclear translocation in microglia. (A) Representative immunofluorescence images showing nuclear staining of transcription factors NFAT and NF- κ B following LPS activation, which is prevented by the CRAC channel inhibitor (CM+). (B) Counts of nuclear stained cells normalized to the total number of NFAT or nuclear factor kappa B (NF- κ B) positive cells per randomly chosen non-overlapping high power field show increased nuclear staining after LPS exposure and inhibition by CM-EX-137 treatment. Bars represent five fields per experiment. Each experiment was repeated three times. (C,D) Representative Western blots of nuclear extracts showing NFAT (C) and NF- κ B (D) from LPS-activated BV2 cells. The CM+ treatment reduced nuclear protein expression of both transcription factors. Histone (HIS), a housekeeping protein in the nucleus, is shown as a control. LPS (LPS treatment alone), CM+ (LPS + CM-EX-137, shown are two separate treatment lanes), CON (control). ($p < 0.01$ * vs. control, # vs. LPS). DAPI, 4',6-diamidino-2-phenylindole.

met criteria for activated microglia based on morphological changes.²⁹ These criteria included increased immunomarker staining plus rounded amoeboid morphology or shortening of processes and enlargement of the cell soma. For CCI, positive cells were counted in five randomly chosen, non-overlapping high-power fields from the perimeter of brain injury, as delineated by the cresyl violet-stained sections. For the LPS-treated animals, inflammatory brain regions were also selected and counted from five non-overlapping fields from both lateral cortices. The percentage of positive cells was normalized to the total number of cells within a given field. For double labeling, numbers of double-labeled cells were normalized to the phenotype marker, CD11b, to identify microglia.

Statistics and rigor

Analysis of variance and *t* test were used for the comparison of three or two experimental groups, respectively. Statistical analyses

were performed using SPSS 23.0 (SPSS, Inc., Chicago, IL). The significance level was set at $p < 0.05$. Animals were randomized to the experimental groups, and all assessments were performed by investigators who were blinded to treatment assignments.

Results

CRAC channel inhibition

CRAC channel inhibition suppresses microglial activation. The BV2 microglial cells were characterized for the presence of CRAC channel components. As expected, BV2 cells expressed both CRAC channel components, STIM1 and Orai1 (Fig. 2A). STIM1 and Orai1 expression, the canonical CRAC channel protein, was unaffected by activation with various microglial activators. A marker of inflammation, iNOS, was increased by activators, but was decreased by treatment with CM-EX-137. The

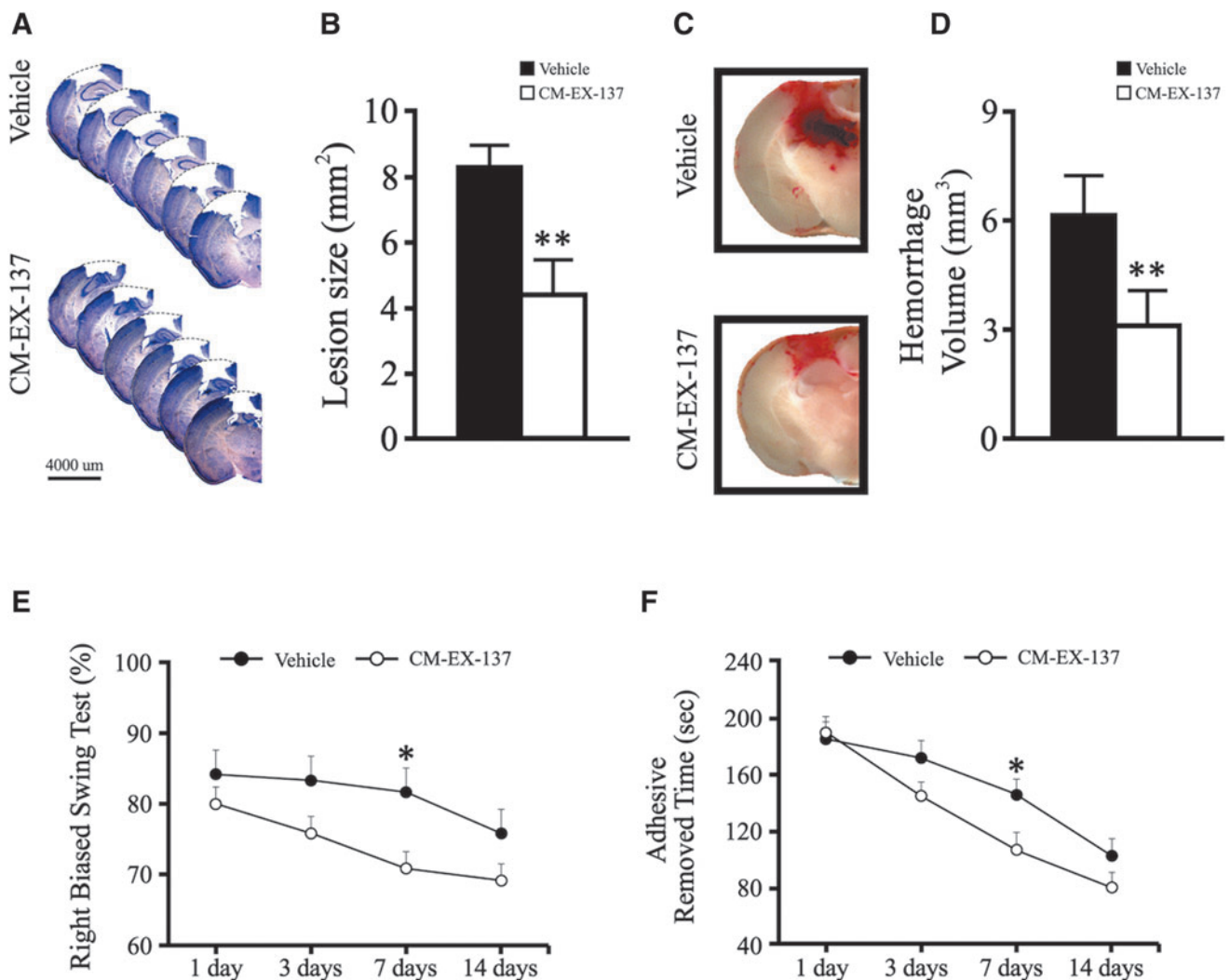


FIG. 4. Calcium release-activated calcium (CRAC) channel inhibition reduces lesion size and brain hemorrhage while improving neurological function. (A) Representative cresyl violet-stained brain sections 14 days post-controlled cortical impact (CCI) are shown in vehicle and CM-EX-137 treated mice. (B) Lesion size was significantly decreased among CM-EX-137 treated mice. Average area occupied by the centermost sections of the lesions are shown (** $p < 0.01$). (C) Gross brain sections show hemorrhage after CCI from vehicle and CM-EX-137 treated mice. Brains were collected three days after CCI. (D) Hemorrhage volume was significantly decreased among CM-EX-137 treated mice (** $p < 0.01$). (E,F) Elevated body swing (E) and adhesive removal tests (F) were performed before operation and one, three, seven, and 14 days after CCI. Decreased right-biased swing and shorter adhesive removal times indicate improved sensorimotor function. The CM-EX-137 treatment improved sensorimotor function compared with vehicle at seven days (black circles: vehicle, white circles: CM-EX-137; * $p < 0.05$).

CM-EX-137 also inhibited agonist-induced elevations in NO in a dose-dependent manner (Fig. 2B–D). Intracellular Ca^{2+} concentration was determined by live cell fluorescence microscopy using a calcium-sensing fluorescent probe (Fig. 2E). Microglial stimulation by LPS led to an increase in intracellular Ca^{2+} concentration,³⁰ consistent with previous data, and this increase was prevented by treatment with CM-EX-137.

The transcription factors NF- κ B and NFAT are activated in inflammatory cells in response to a variety of immune stimuli. Opening of CRAC channels facilitates the entry of calcium that activates NFAT in lymphocytes. To determine whether the same occurs in microglia, we stimulated BV2 cells with LPS and observed activation of both NFAT and NF- κ B, as evidenced by an increase in their nuclear staining (Fig. 3A,B). Treatment with CM-EX-137 reduced this nuclear staining. Western blots of nuclear extracts also showed that CRAC channel inhibition reduced nuclear localization of both NFAT (Fig. 3C) and NF- κ B (Fig. 3D).

CRAC channel inhibition reduces brain hemorrhage and lesion size. In the CCI model, all mice survived for three days or 14 days, and there were no unanticipated deaths. Lesion volume was significantly decreased in the CM-EX-137-treated group compared with vehicle injected mice (Fig. 4A,B). Hemorrhage volume ($p < 0.01$) was decreased significantly among CM-EX-137 treated mice compared with vehicle treated animals (Fig. 4C,D).

CRAC channel inhibition improves neurological outcome after CCI. Elevated body swing and adhesive removal tests were performed on days one, three, seven, and 14 after CCI. These tests were also performed before operation, and there were no significant differences between the two groups. Both behavioral indices were significantly improved in mice treated with CM-EX-137 compared with the vehicle injected mice group at seven days post-CCI (Fig. 4E,F). Decreased right-biased swings and shorter adhesive removal times indicated improvements in motor function. Contact times from the adhesive removal test, however, were no different between groups (data not shown) and suggest that sensory function was less impacted by treatment compared with motor function. These results suggest that CRAC channel inhibition also improved neurological function.

CRAC channel inhibition decreased numbers of activated microglia after CCI and in a model of brain inflammation. Among mice exposed to CCI, the number of activated microglia as assessed by morphological changes (enlargement of the cell body, thickening and retraction of processes) and intense isolectin B4 staining was significantly decreased in mice treated with CM-EX-137 compared with vehicle (Fig. 5A,B, $p < 0.001$). Similarly, mice treated with LPS to cause brain inflammation without brain cell injury had increased microglial activation, which was suppressed by CM-EX-137 treatment (Fig. 5C,D).

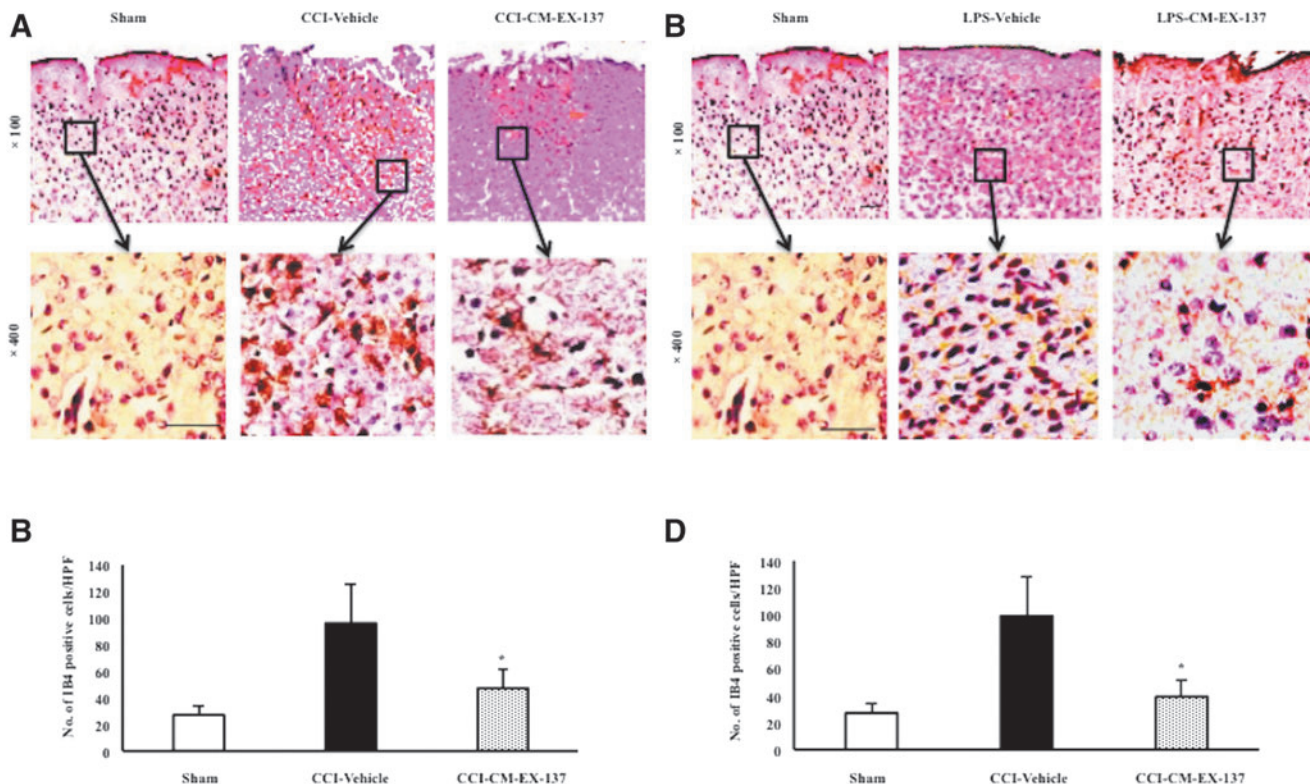


FIG. 5. Calcium release-activated calcium (CRAC) channel inhibition decreased numbers of activated microglia/macrophages after controlled cortical impact (CCI) and lipopolysaccharide (LPS) exposure. Isolectin B4 (IB4) was used to identify microglia and other myeloid cells such as macrophages and monocytes. The CCI increased the intensity of IB4 staining, and CM-EX-137 decreased the CCI response three days post-CCI (A). Cell counts were sampled at the lesion border. The number of activated microglia/macrophages/monocytes as evidenced by morphological change and increased IB4 staining was increased by CCI and reduced by CRAC channel inhibition ($*p < 0.001$) (B). Similar patterns were observed in the LPS brain inflammation model (C,D) ($*p < 0.001$). CCI, mice received traumatic brain injury; vehicle, received vehicle treatment; CM-EX-137, received CRAC channel inhibitor treatment; LPS, received LPS to model brain inflammation; sham, no insult, no treatment; scale bar, $5 \mu\text{m}$ ($\times 100$) and $20 \mu\text{m}$ ($\times 400$).

THE CD68 (Fig. 6), used to identify phagocytic cells including activated microglia and circulating macrophages, and iNOS (Fig. 7), a marker of pro-inflammatory activation, were both increased by CCI, and reduced by treatment with CM-EX-137. These effects were confirmed in the LPS neuroinflammation model. These observations indicate that CRAC channel inhibition leads to suppression of inflammation.

CRAC channel inhibition reduced numbers of STIM1 and Orai1 positive microglia. To characterize the effects of CCI on STIM1 and Orai1, we probed adjacent sections for the presence of these proteins. The CCI upregulated both STIM1 (Fig. 8A) and Orai1 (Fig. 8D). Total numbers of STIM1 and Orai1 positive cells were not different among the CCI groups, indicating that CRAC channel inhibition did not alter total numbers of cells that expressed these proteins. Total numbers of microglia/macrophages (identified by CD11b staining) were decreased, however, in mice treated with CM-EX-137, and the proportion of these cells that were also positive for STIM1 and Orai1 was decreased in the treated group (Fig. 8B,C, E,F). This would suggest that CM-EX-137 may inhibit CRAC channels preferentially on microglia/macrophages.

Discussion

Inflammation after brain ischemia is known to contribute negatively to outcome. Over the years, strategies to limit these immune responses have been shown to improve neurological outcomes after experimental brain trauma.² It has been recognized recently that the CRAC channel participates in the activation of immune responses in the brain. Components of this channel include STIM1 and Orai1.^{6,7,31-33} The STIM1 protein is found within the ER, where it can detect changes in luminal calcium. Orai1 resides in the plasma membrane and is the pore-forming unit of the CRAC channel. Calcium levels in the ER are decreased after stimulation of a number of immune receptors, including, as shown in the *in vitro* studies, Toll-like receptors-3 (TLR3, activated by PIC) and -4 (TLR4, activated by LPS). Decreased ER Ca^{2+} causes STIM1 to oligomerize and translocate to ER regions closely apposed to the plasma membrane, where it binds to and gates Orai1, leading to Ca^{2+} influx through the channel.³⁴⁻³⁶

The CRAC channel has been observed on lymphocytes and mast cells, but also on microglia.^{4,5} Elevated intracellular calcium levels activate calcineurin, which then activates NFAT. The NFAT, much like NF- κ B, resides in the cytosol in the resting state and after

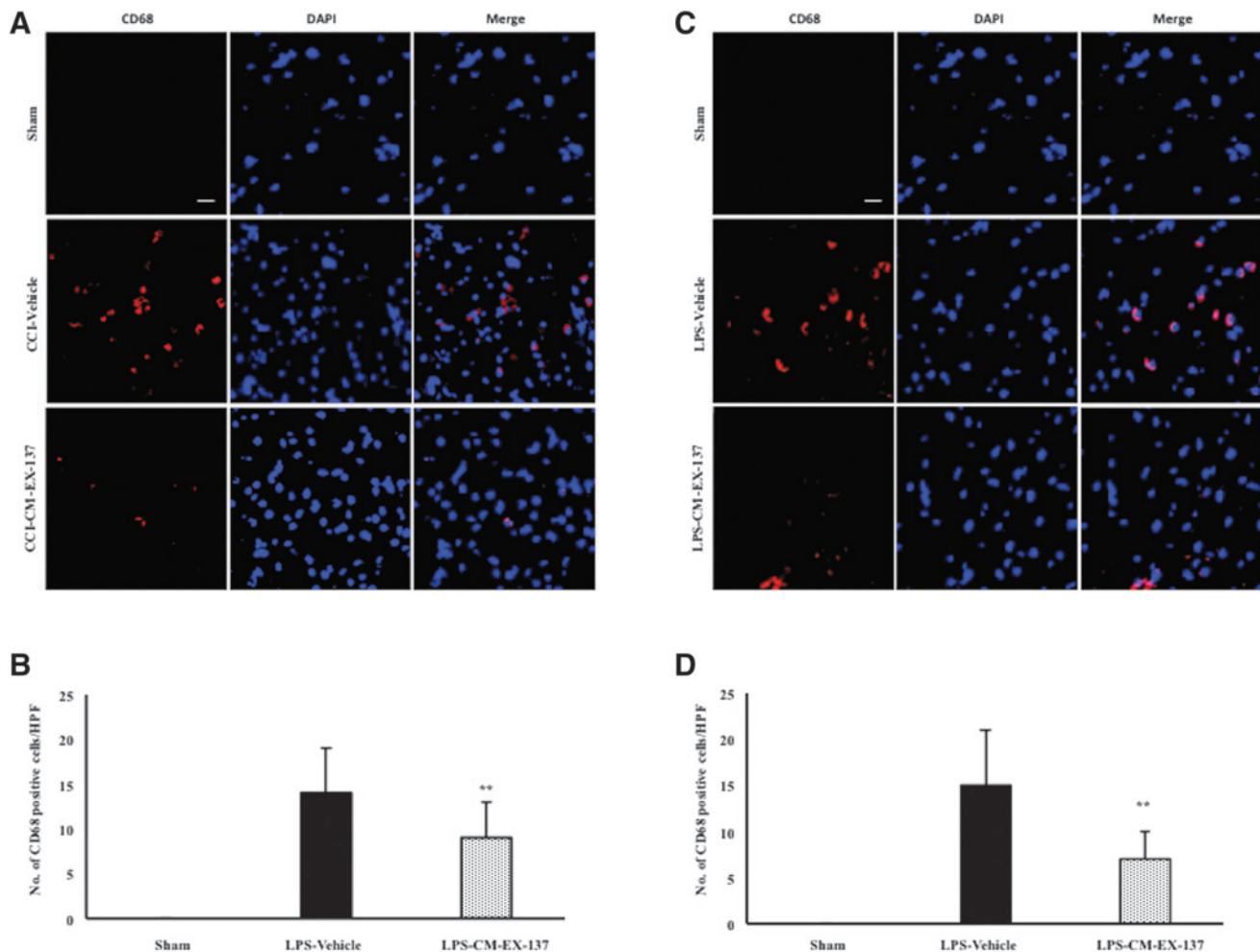


FIG. 6. Calcium release-activated calcium (CRAC) channel inhibition decreased numbers of CD68 positive cells. The CD68 was used to identify phagocytic cells, including brain and circulating macrophages. At three days post-CCI, these cells were observed mostly in the periphery of the brain lesion, and their numbers were decreased by CM-EX-137 treatment (A). Counts of positive cells sampled from this region showed significant reduction with treatment (B). Similar patterns emerged in a model of brain inflammation induced by lipopolysaccharide (LPS) (C,D). Brains were collected one day post-LPS administration. (** $p < 0.01$; scale bar, 20 μ m).

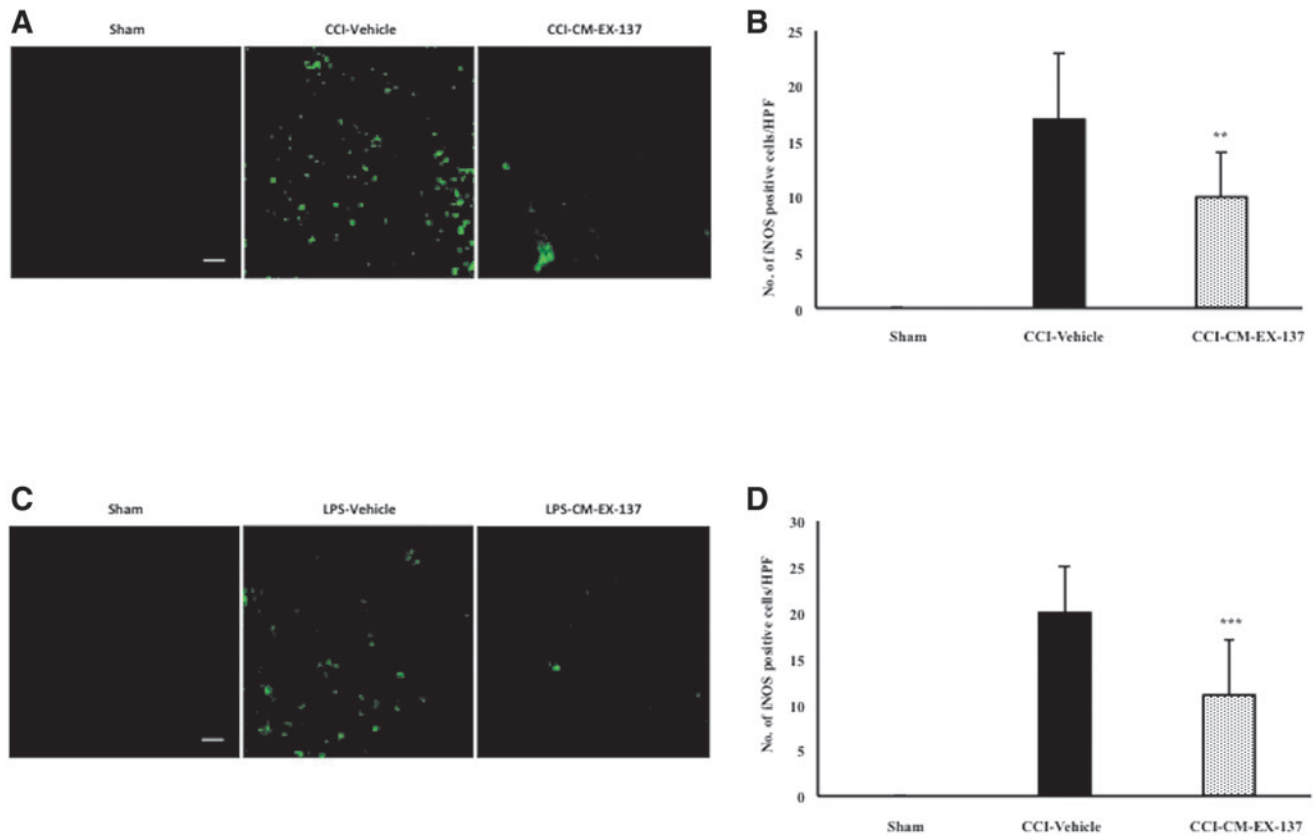


FIG. 7. Calcium release-activated calcium (CRAC) channel inhibition decreased numbers of inducible nitric oxide synthase (iNOS) positive cells. Immunofluorescence stains of iNOS after controlled cortical impact (CCI) (**A,B**) and lipopolysaccharide (LPS)-induced neuroinflammation (**C,D**) showed that both insults increased iNOS expression. In both models, treatment with CM-EX-137 led to significant reduction of iNOS positive cells. (** $p < 0.01$; *** $p < 0.005$; scale bar, 20 μm).

activation is de-phosphorylated by calcineurin, allowing it to translocate to the nucleus where it upregulates several genes encoding pro-inflammatory molecules (Fig. 1).³⁷ Further, both STIM1 and Orai1 have been reported to be upregulated by the glucocorticoid-inducible kinase SGK1-dependent NF- κ B signaling at the messenger ribonucleic acid and protein levels.³⁸

In this study, both STIM1 and Orai1 were upregulated after LPS injection and CCI, which may have been induced via NF- κ B. Our *in vitro* data indicate the CM-EX-137 also suppressed nuclear NF- κ B translocation. Hence, inhibition of this cycle by CM-EX-137 decreased both STIM1 and Orai1 along with suppression of microglial activation.

Recent studies in stroke, TBI, and multiple sclerosis models showed that gene deletion of the CRAC channel component protein STIM1 led to favorable outcomes.^{39–41} While inflammation in brain trauma has been studied for some time, only a few studies have explored specifically the role of CRAC channels. A few laboratories have studied the effects of gene knockdown/deletion of CRAC channel components,^{39–43} and there are several studies involving CNIs,^{12,44} but those that are available clinically are not specific and have toxicities as well.^{18,19,45–47} In fact, a recent pre-clinical study by Operation Brain Trauma Therapy⁴⁸ indicated a narrow therapeutic window for CsA in the management of brain trauma. While investigators observed neuroprotection at a low dose in some, but not all experimental models, it was actually deleterious at higher doses. This is not surprising, because there is ample clinical evidence of low therapeutic windows with CNIs in the

prevention of organ transplant rejection and autoimmune diseases.⁴⁹ Chronic use of these compounds also leads to nephrotoxicity and neurotoxicity, which limits their wide use.^{18,19}

Nevertheless, CsA was studied in a small stroke treatment trial of 127 patients, but no efficacy was demonstrated.⁵⁰ CsA and FK506 are not very specific, in that they can regulate other calcium channels and have been shown to affect mitochondria.^{51,52} From the pharmacological data by CalciMedica, CM-EX-137 displayed no activity on other receptors and a variety of ion channels (Supplementary Tables 1 and 2; see online supplementary material at <http://www.liebertpub.com>). This may be one reason to explain the safety of CM-EX-137 compared with existing CNIs; however, like all drugs, adverse effects of CM-EX-137 can be seen at high doses. In fact, pre-clinical studies showed that at the very highest doses tested, weight loss in animals can develop. Regardless, there may be advantages to studying inhibitors that lack the side effects of existing CNIs. Further, CNIs have only demonstrated anti-inflammatory effects via inhibition of calcineurin and suppression of NFAT. We showed that CRAC channel inhibition inhibited microglial activation by preventing upstream calcium influx, which may not occur with existing CNIs.

CalciMedica is developing small molecule CRAC channel inhibitors that inhibit Orai1-containing CRAC channels, and pre-clinical studies have indicated that the pharmacological and toxicological profiles of their CRAC channel inhibitors are different compared with CNIs. Pilot *in vitro* studies in our laboratory showed that CM-EX-137 demonstrated the most robust microglial inhibiting

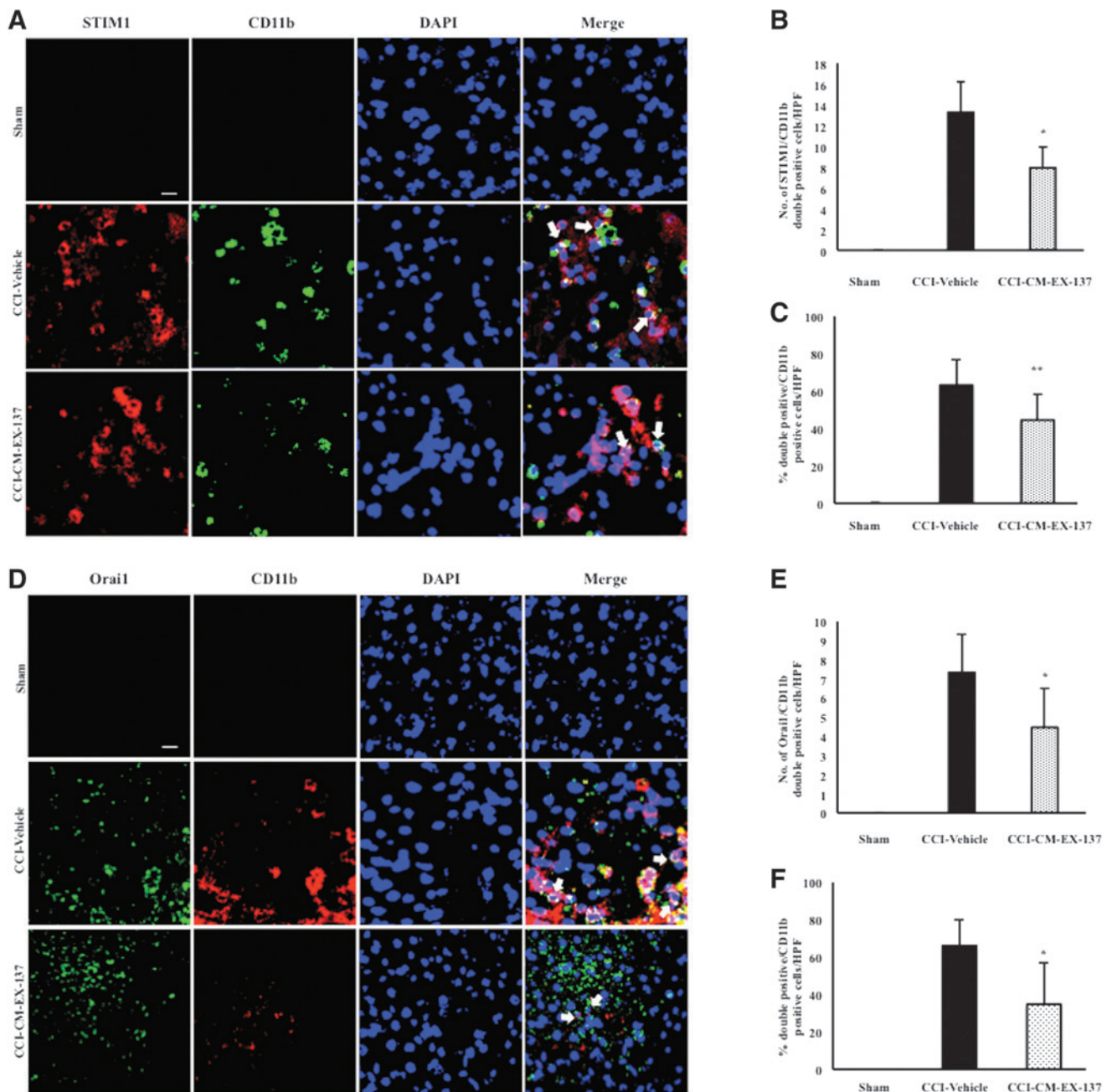


FIG. 8. Calcium release-activated calcium (CRAC) channel components stromal interaction molecule-1 (STIM1) and Orai1 increase after controlled cortical impact (CCI), and are suppressed in CD11b positive cells by CM-EX-137 treatment. Double immunofluorescent staining three days post-CCI for the myeloid cell marker CD11b and STIM1 (A–C) or Orai1 (D–F) are shown. Both CRAC channel components increased after CCI (CCI-vehicle rows), but CM-EX-137 treatment did not affect total numbers of positive cells (CCI-CM-EX-137 rows). Counts of double positive cells (merge columns), however, showed that CM-EX-137 reduced numbers of both STIM1 (B) and Orai1 (E) positive cells that were also CD11b positive. Because CM-EX-137 treatment also reduced total numbers of CD11b positive cells, we then expressed our counts as the percentage of CD11b positive cells, and similar patterns emerged (C,F). This suggests that CM-EX-137 may preferentially inhibit CRAC channel expression on microglial cells (* $p < 0.001$, ** $p < 0.01$; arrows indicate representative double positive cells; scale bar, 20 μm).

properties of several CalciMedica molecules evaluated and did not cause increased neuronal death. We demonstrate here that this novel, selective CRAC channel inhibitor is capable of inhibiting microglial activation and, as such, improved outcomes and reduced brain hemorrhage and inflammation in an experimental model of TBI. As further evidence of the mechanism that is reducing brain inflam-

mation, we show in *in vitro* and *in vivo* models of brain inflammation that this inhibitor directly suppresses microglial activation.

It bears mentioning that although we observed significantly improved sensorimotor function only at seven days post-CCI, this effect was no longer statistically significant by 14 days. Inspection of our data indicates that this is likely because of the spontaneous

improvement displayed by the vehicle-treated control group. This is not unexpected and has been observed by other groups using similar assessments, including our own.²⁷ While this could be interpreted as a transient effect of treatment, it more likely reflects the inability of our behavioral assessments to detect subtle differences in function. Yet, histological studies indicate that lesion volume was nonetheless decreased among treated animals. Future studies should investigate more sensitive assays, including those that assess cognitive function, a common yet underappreciated complication of TBI, as well as other biomarkers.

Pilot data from CalciMedica demonstrated a brain:plasma ratio of about 4–5 for CM-EX-137 after oral dosing, and the IP dose in the current study was selected based on plasma pharmacokinetic data after IP dosing and extrapolation to brain levels that correlated with the inhibition of microglial activation in our *in vitro* model. Daily dosing was maintained for 7 days, because our previous studies in a related stroke model have shown that microglia are activated within hours of ischemia onset and peak numbers of activated microglia are seen by about day 7.^{23,29} This time course appears to be similar in models of TBI as well.⁵³ We delivered the compound parenterally, because patients with acute neurological insults often present with impaired swallowing mechanisms or even coma. Oral formulations of this compound are available, however, and could be used with patients whose swallowing functions are not compromised. This opens the possibility of applications beyond brain injury, including chronic neurological disorders.

Conclusion

The study of small molecule CRAC channel inhibitors for the management of acute neurological injury is a new area of investigation, and we demonstrate for the first time that they may have a role in the management of acute brain trauma. The CRAC channel inhibitors are already being studied in humans as a potential therapy in immune, cancer, and acute inflammatory conditions, but have not been studied for diseases of the brain. This work may inspire future investigations for management of related neurological conditions.

Acknowledgments

This work was supported by grants from the Veterans Affairs Merit Award I01 BX000589 and NIH National Institute of Neurological Disorders and Stroke R03 NS101246, and gift funds from CalciMedica, Inc (to MY) and the SENSHIN Medical Research Foundation (to AM). Grants to MY were administered by the Northern California Institute for Research and Education, and supported by resources from the Veterans Affairs Medical Center, San Francisco, CA.

Author Disclosure Statement

Authors Stauderman, Dunn, and Hebbar are employed by CalciMedica and are also stockholders in the company. They have also filed a patent for the CM-EX-137 compound for “using of CRAC channel inhibitors for the treatment of stroke and traumatic brain injury.” For the remaining authors, no competing financial interests exist.

References

- Iadecola, C. and Anrather, J. (2011). The immunology of stroke: from mechanisms to translation. *Nat. Med.* 17, 796–808.
- Corps, K.N., Roth, T.L., and McGavern, D.B. (2015). Inflammation and neuroprotection in traumatic brain injury. *JAMA Neurol.* 72, 355–362.
- Kraft, R. (2015). STIM and ORAI proteins in the nervous system. *Channels (Austin)* 9, 245–252.
- Beck, A., Penner, R., and Fleig, A. (2008). Lipopolysaccharide-induced down-regulation of Ca²⁺ release-activated Ca²⁺ currents (I CRAC) but not Ca²⁺-activated TRPM4-like currents (I CAN) in cultured mouse microglial cells. *J. Physiol.* 586, 427–439.
- Ohana, L., Newell, E.W., Stanley, E.F., and Schlichter, L.C. (2009). The Ca²⁺ release-activated Ca²⁺ current (I(CRAC)) mediates store-operated Ca²⁺ entry in rat microglia. *Channels (Austin)* 3, 129–139.
- Roos, J., DiGregorio, P.J., Yeromin, A.V., Ohlsen, K., Lioudyno, M., Zhang, S., Safrina, O., Kozak, J.A., Wagner, S.L., Cahalan, M.D., Velicelebi, G., and Stauderman, K.A. (2005). STIM1, an essential and conserved component of store-operated Ca²⁺ channel function. *J. Cell Biol.* 169, 435–445.
- Zhang, S.L., Yu, Y., Roos, J., Kozak, J.A., Deerinck, T.J., Ellisman, M.H., Stauderman, K.A., and Cahalan, M.D. (2005). STIM1 is a Ca²⁺ sensor that activates CRAC channels and migrates from the Ca²⁺ store to the plasma membrane. *Nature* 437, 902–905.
- Shim, A.H., Tirado-Lee, L., and Prakriya, M. (2015). Structural and functional mechanisms of CRAC channel regulation. *J. Mol. Biol.* 427, 77–93.
- Furman, J.L. and Norris, C.M. (2014). Calcineurin and glial signaling: neuroinflammation and beyond. *J. Neuroinflammation* 11, 158.
- Cho, T.H., Aguetaz, P., Campuzano, O., Charriaut-Marlangue, C., Riou, A., Berthezene, Y., Nighoghossian, N., Ovize, M., Wiart, M., and Chauveau, F. (2013). Pre- and post-treatment with cyclosporine A in a rat model of transient focal cerebral ischaemia with multimodal MRI screening. *Int. J. Stroke* 8, 669–674.
- Kuroda, S., Janelidze, S., and Siesjo, B.K. (1999). The immunosuppressants cyclosporin A and FK506 equally ameliorate brain damage due to 30-min middle cerebral artery occlusion in hyperglycemic rats. *Brain Res.* 835, 148–153.
- Osman, M.M., Lulic, D., Glover, L., Stahl, C.E., Lau, T., van Loveren, H., and Borlongan, C.V. (2011). Cyclosporine-A as a neuroprotective agent against stroke: its translation from laboratory research to clinical application. *Neuropeptides* 45, 359–368.
- Furuichi, Y., Maeda, M., Matsuoka, N., Mutoh, S., and Yanagihara, T. (2007). Therapeutic time window of tacrolimus (FK506) in a nonhuman primate stroke model: comparison with tissue plasminogen activator. *Exp. Neurol.* 204, 138–146.
- Macleod, M.R., O’Collins, T., Horky, L.L., Howells, D.W., and Donnan, G.A. (2005). Systematic review and metaanalysis of the efficacy of FK506 in experimental stroke. *J. Cereb. Blood Flow Metab.* 25, 713–721.
- Marmarou, C.R. and Povlishock, J.T. (2006). Administration of the immunophilin ligand FK506 differentially attenuates neurofilament compaction and impaired axonal transport in injured axons following diffuse traumatic brain injury. *Exp. Neurol.* 197, 353–362.
- Gold, B.G., Voda, J., Yu, X., McKeon, G., and Bourdette, D.N. (2004). FK506 and a nonimmunosuppressant derivative reduce axonal and myelin damage in experimental autoimmune encephalomyelitis: neuroimmunophilin ligand-mediated neuroprotection in a model of multiple sclerosis. *J. Neurosci. Res.* 77, 367–377.
- Singleton, R.H., Stone, J.R., Okonkwo, D.O., Pellicane, A.J., and Povlishock, J.T. (2001). The immunophilin ligand FK506 attenuates axonal injury in an impact-acceleration model of traumatic brain injury. *J. Neurotrauma* 18, 607–614.
- Bechstein, W.O. (2000). Neurotoxicity of calcineurin inhibitors: impact and clinical management. *Transpl. Int.* 13, 313–326.
- Malvezzi, P. and Rostaing, L. (2015). The safety of calcineurin inhibitors for kidney-transplant patients. *Expert Opin. Drug Saf.* 14, 1531–1546.
- Kacimi, R., Giffard, R.G., and Yenari, M.A. (2011). Endotoxin-activated microglia injure brain derived endothelial cells via NF- κ B, JAK-STAT and JNK stress kinase pathways. *J. Inflamm. (Lond)* 8, 7.
- Kacimi, R. and Yenari, M.A. (2015). Pharmacologic heat shock protein 70 induction confers cytoprotection against inflammation in gliovascular cells. *Glia* 63, 1200–1212.
- Zheng, Z., Kim, J.Y., Ma, H., Lee, J.E., and Yenari, M.A. (2008). Anti-inflammatory effects of the 70 kDa heat shock protein in experimental stroke. *J. Cereb. Blood Flow Metab.* 28, 53–63.
- Han, H.S., Qiao, Y., Karabiyikoglu, M., Giffard, R.G., and Yenari, M.A. (2002). Influence of mild hypothermia on inducible nitric oxide

- synthase expression and reactive nitrogen production in experimental stroke and inflammation. *J. Neurosci.* 22, 3921–3928.
24. Kim, J.Y., Kim, N., Yenari, M.A., and Chang, W. (2013). Hypothermia and pharmacological regimens that prevent overexpression and overactivity of the extracellular calcium-sensing receptor protect neurons against traumatic brain injury. *J. Neurotrauma* 30, 1170–1176.
 25. Deng, H., Han, H.S., Cheng, D., Sun, G.H., and Yenari, M.A. (2003). Mild hypothermia inhibits inflammation after experimental stroke and brain inflammation. *Stroke* 34, 2495–2501.
 26. d'Avila, J.C., Lam, T.I., Bingham, D, Shi, J., Won, S.J., Kauppinen, T.M., Massa, S., Liu J., and Swanson, R.A. (2012). Microglial activation induced by brain trauma is suppressed by post-injury treatment with a PARP inhibitor. *J. Neuroinflammation* 9, 31.
 27. Kim, N., Kim, J.Y., and Yenari, M.A. (2015). Pharmacological induction of the 70-kDa heat shock protein protects against brain injury. *Neuroscience* 284, 912–919.
 28. Tang, X.N., Berman, A.E., Swanson, R.A., and Yenari, M.A. (2010). Digitally quantifying cerebral hemorrhage using Photoshop and Image J. *J. Neurosci. Methods* 190, 240–243.
 29. Wang, G.J., Deng, H.Y., Maier, C.M., Sun, G.H., and Yenari, M.A. (2002). Mild hypothermia reduces ICAM-1 expression, neutrophil infiltration and microglia/monocyte accumulation following experimental stroke. *Neuroscience* 114, 1081–1090.
 30. Hoffmann, A., Kann, O., Ohlemeyer, C., Hanisch, U.K., and Kettenmann, H. (2003). Elevation of basal intracellular calcium as a central element in the activation of brain macrophages (microglia): suppression of receptor-evoked calcium signaling and control of release function. *J. Neurosci.* 23, 4410–4419.
 31. Prakriya, M. and Lewis, R.S. (2015). Store-operated calcium channels. *Physiol. Rev.* 95, 1383–1436.
 32. Vig, M., Beck, A., Billingsley, J.M., Lis, A., Parvez, S., Peinelt, C., Koomoa, D.L., Soboloff, J., Gill, D.L., Fleig, A., Kinet, J.P., and Penner, R. (2006). CRACM1 multimers form the ion-selective pore of the CRAC channel. *Curr. Biol.* 16, 2073–2079.
 33. Liou, J., Kim, M.L., Heo, W.D., Jones, J.T., Myers, J.W., Ferrell, J.E., Jr., and Meyer, T. (2005). STIM is a Ca²⁺ sensor essential for Ca²⁺-store-depletion-triggered Ca²⁺ influx. *Curr. Biol.* 15, 1235–1241.
 34. Cahalan, M.D., Zhang, S.L., Yeromin, A.V., Ohlsen, K., Roos, J., and Stauderman, K.A. (2007). Molecular basis of the CRAC channel. *Cell Calcium* 42, 133–144.
 35. Feske, S., Gwack, Y., Prakriya, M., Srikanth, S., Puppel, S.H., Tanasa, B., Hogan, P.G., Lewis, R.S., Daly, M., and Rao, A. (2006). A mutation in Orai1 causes immune deficiency by abrogating CRAC channel function. *Nature* 441, 179–185.
 36. Prakriya, M., Feske, S., Gwack, Y., Srikanth, S., Rao, A., and Hogan, P.G. (2006). Orai1 is an essential pore subunit of the CRAC channel. *Nature* 443, 230–233.
 37. Rao, A., Luo, C., and Hogan, P.G. (1997). Transcription factors of the NFAT family: regulation and function. *Annu. Rev. Immunol.* 15, 707–747.
 38. Eylenstein, A., Schmidt, S., Gu, S., Yang, W., Schmid, E., Schmidt, E.M., Alesutan, I., Szteyn, K., Regel, I., Shumilinam, E., and Lang, F. (2012). Transcription factor NF- κ B regulates expression of pore-forming Ca²⁺ channel unit, Orai1, and its activator, STIM1, to control Ca²⁺ entry and affect cellular functions. *J. Biol. Chem.* 287, 2719–2730.
 39. Berna-Ero, A., Braun, A., Kraft, R., Kleinschnitz, C., Schuhmann, M.K., Stegner, D., Wultsch, T., Eilers, J., Meuth, S.G., Stoll, G., and Nieswandt, B. (2009). STIM2 regulates capacitive Ca²⁺ entry in neurons and plays a key role in hypoxic neuronal cell death. *Sci. Signal.* 2, ra67.
 40. Ma, J., McCarl, C.A., Khalil, S., Luthy, K., and Feske, S. (2010). T-cell-specific deletion of STIM1 and STIM2 protects mice from EAE by impairing the effector functions of Th1 and Th17 cells. *Eur. J. Immunol.* 40, 3028–3042.
 41. Rao, W., Zhang, L., Peng, C., Hui, H., Wang, K., Su, N., Wang, L., Dai, S.H., Yang, Y.F., Chen, T., Luo, P., and Fei, Z. (2015). Down-regulation of STIM2 improves neuronal survival after traumatic brain injury by alleviating calcium overload and mitochondrial dysfunction. *Biochim. Biophys. Acta* 1852, 2402–2413.
 42. Hou, P.F., Liu, Z.H., Li, N., Cheng, W.J., and Guo, S.W. (2015). Knockdown of STIM1 improves neuronal survival after traumatic neuronal injury through regulating mGluR1-dependent Ca²⁺ signaling in mouse cortical neurons. *Cell Mol. Neurobiol.* 35, 283–292.
 43. Heo, D.K., Lim, H.M., Nam, J.H., Lee, M.G., and Kim, J.Y. (2015). Regulation of phagocytosis and cytokine secretion by store-operated calcium entry in primary isolated murine microglia. *Cell Signal.* 27, 177–186.
 44. Saganova, K., Galik, J., Blasko, J., Korimova, A., Racekova, E., and Mingeova, I. (2012). Immunosuppressant FK506: focusing on neuroprotective effects following brain and spinal cord injury. *Life Sci.* 91, 77–82.
 45. Servais, H., Ortiz, A., Devuyst, O., Denamur, S., Tulkens, P.M., and Mingot-Leclercq, M.P. (2008). Renal cell apoptosis induced by nephrotoxic drugs: cellular and molecular mechanisms and potential approaches to modulation. *Apoptosis* 13, 11–32.
 46. Christians, U., Gottschalk, S., Miljus, J., Hainz, C., Benet, L.Z., Leibfritz, D., and Serkova, N. (2004). Alterations in glucose metabolism by cyclosporine in rat brain slices link to oxidative stress: interactions with mTOR inhibitors. *Br. J. Pharmacol.* 143, 388–396.
 47. Serkova, N.J., Christians, U., and Benet, L.Z. (2004). Biochemical mechanisms of cyclosporine neurotoxicity. *Mol. Interv.* 4, 97–107.
 48. Dixon, C.E., Bramlett, H.M., Dietrich, W.D., Shear, D.A., Yan, H.Q., Deng-Bryant, Y., Mondello, S., Wang, K.K., Hayes, R.L., Empey, P.E., Povlishock, J.T., Tortella, F.C., and Kochanek, P.M. (2016). Cyclosporine treatment in traumatic brain injury: operation brain trauma therapy. *J. Neurotrauma* 33, 553–566.
 49. Siekierka, J.J. and Sigal, N.H. (1992). FK-506 and cyclosporin A: immunosuppressive mechanism of action and beyond. *Curr. Opin. Immunol.* 4, 548–552.
 50. Nighoghossian, N., Berthezene, Y., Mechtouff, L., Derex, L., Cho, T.H., Ritzenthaler, T., Rheims, S., Chauveau, F., Bejot, Y., Jacquin, A., Giroud, M., Ricolfi, F., Philippeau, F., Lamy, C., Turc, G., Bodiguel, E., Domingo, V., Guiraud, V., Mas, J.L., Oppenheim, C., Amarenco, P., Cakmak, S., Sevin-Allouet, M., Guillon, B., Desal, H., Hosseini, H., Sibon, I., Mahagne, M.H., Ong, E., Mewton, N., and Ovize, M. (2015). Cyclosporine in acute ischemic stroke. *Neurology* 84, 2216–2223.
 51. Furuichi, Y., Noto, T., Li, J.Y., Oku, T., Ishiye, M., Moriguchi, A., Aramori, I., Matsuoka, N., Mutoh, S., and Yanagihara, T. (2004). Multiple modes of action of tacrolimus (FK506) for neuroprotective action on ischemic damage after transient focal cerebral ischemia in rats. *Brain Res.* 1014, 120–130.
 52. Kaminska, B., Gaweda-Walerych, K., and Zawadzka, M. (2004). Molecular mechanisms of neuroprotective action of immunosuppressants—facts and hypotheses. *J. Cell Mol. Med.* 8, 45–58.
 53. Chiu, C.C., Liao, Y.E., Yang, L.Y., Wang, J.Y., Tweedie, D., Karnati, H.K., Greig, N.H., and Wang, J.Y. (2016). Neuroinflammation in animal models of traumatic brain injury. *J. Neurosci. Methods* 272, 38–49.

Address correspondence to:

Midori A. Yenari, MD

Department of Neurology

University of California, San Francisco

San Francisco VAMC

4150 Clement Street, MS 127

San Francisco, CA 94121

E-mail: yenari@alum.mit.edu